Experimental Modal Substructuring to Couple and Uncouple Substructures with Flexible Fixtures and Multi-point Connections

Matthew S. Allen*,
Assistant Professor, University of Wisconsin-Madison, Department of Engineering Physics
535 Eng. Research Building, 1500 Engineering Drive, Madison, Wisconsin 53706-1609

Randall L. Mayes &
Distinguished Member of Technical Staff, MS 0557
Sandia National Laboratories, P.O. Box 5800, Albuquerque, New Mexico 87185

Elizabeth J. Bergman
Instructor, Madison Area Technical College
3550 Anderson Street, Madison, Wisconsin 53704

Abstract

Modal substructuring or Component Mode Synthesis (CMS) has been standard practice for many decades in the analytical realm, yet a number of significant difficulties have been encountered when attempting to combine experimentally derived modal models with analytical ones or when predicting the effect of structural modifications using experimental measurements. This work presents a new method that removes the effects of a flexible fixture from an experimentally obtained modal model. It can be viewed as an extension to the approach where rigid masses or massless springs are removed from a structure. The approach presented here improves the modal basis of the substructure, so that it can be used to more accurately estimate the modal parameters of the built-up system. New types of constraints are also presented, which constrain the modal degrees of freedom of the substructures, avoiding the need to estimate the connection point displacements and rotations. These constraints together with the use of a flexible fixture enable a new approach for joining structures, especially those with statically-indeterminate multi-point connections, such as two circular flanges that are joined by many more bolts than required to enforce compatibility if the substructures were rigid. Fixture design is discussed, one objective of which is to achieve a mass-loaded boundary condition that exercises the substructure at the connection point as it is in the built up system. The proposed approach is demonstrated with

* Corresponding Author: msallen@engr.wisc.edu, tel. +1-608-890-1619, fax. +1-608-263-7451

two examples using experimental measurements from laboratory systems. The first is a simple problem of joining two beams of differing lengths, while the second consists of a three-dimensional structure comprising a circular plate that is bolted at eight locations to a flange on a cylindrical structure. In both cases frequency response functions predicted by the substructuring methods agree well with those of the actual coupled structures over a significant range of frequencies.

Keywords:

Modal Constraints for Fixture and Subsystem (MCFS); Craig-Bampton; Mass-loaded interface; Admittance; Impedance

Nomenclature:

$\mathbf{M}$, $\mathbf{C}$, $\mathbf{K}$ – Mass, damping and stiffness matrices

$\mathbf{x}$ – vector of generalized displacement coordinates

$\mathbf{y}$ – vector of physical displacements

$\mathbf{q}$ – vector of modal displacements

$\mathbf{x}_u$ – vector of unconstrained generalized coordinates

$\mathbf{F}$ – vector of applied forces

$\mathbf{\Phi}$ – mass normalized mode shape matrix

ω_r – natural frequency

ζ – modal damping ratio

$\mathbf{a}$ – matrix of constraints in modal coordinates

$\mathbf{a}_p$ – matrix of constraints in physical coordinates

$\mathbf{y}_{A,CPT}$ – vector of physical displacements of subsystem A at the connection degrees of freedom.

$\mathbf{y}_{A,m}$ – vector of physical displacements of subsystem A at the measurement points.

$[\ ]^{\dagger}$ – Moore-Penrose pseudo-inverse of $[\ ]$

1. Introduction

Modern structures are typically designed by groups of engineers, each of which is primarily responsible for a particular subsystem. The dynamic performance of the structure depends on how all of these subsystems interact, yet some of them may be very difficult to model adequately. For example, a company that designs automotive seats is probably not interested in modeling the entire structure of each of the automobiles in which their seats may be used, especially considering the complexity of the automobile due to its intricate geometry, joints with unknown properties, variety of materials, unknown damping effects, and the potential for nonlinearity. However, that complicated structure strongly affects the performance of their seats as experienced by a consumer. Experimental substructuring could allow one to instead create an experimental model for the automobile through test and then couple that experimental model to analytical models of the seats to predict the performance of the built-up structure. Numerous other applications could be mentioned in a variety of industries.

While subcomponent modeling of built-up structures has become commonplace using finite elements, direct coupling of experimental and analytical models is rare because of the difficulties encountered. Methods for combining experimental and analytical substructures can be classified in two different groups. Response based methods, also termed impedance coupling [1-3], admittance coupling [4, 5], or structural modification [6-8] operate on the frequency response functions (FRFs) of the subsystems to predict the responses of the coupled system. An excellent review of these methods was recently presented by de Klerk, Rixen and Voormeeren [9], where these methods were all called Frequency-response Based Substructuring (FBS). These methods have also been derived from a controls perspective in, for example, [10] and they have been used fairly widely in electrical engineering. The other approach, called Modal Substructuring (MS) or Experimental Component Mode Synthesis (ECMS or CMS) joins the substructures based on their linear differential equations of motion [1, 11, 12]. The most common of these in the analytical realm is the Craig-Bampton method [13]. This paper focuses on modal substructuring, although a parallel effort has applied these methods to impedance coupling using FRFs [14-16]. That comparison has found that, while the two approaches each provide a valuable perspective on the issues involved, the end results are usually very similar (also see, e.g., [3]).

When modal substructuring is employed it is critical to assure that the modes of the substructures form an adequate basis for the motion of the coupled structure. A number of methods have been proposed to achieve this, including the classical Craig-Bampton approach that uses fixed-interface and constraint modes [13], the use of free

modes with or without residual flexibility [17, 18] or the use of discrete springs at the interfaces [10]. Each of these approaches suffers from some important experimental difficulties, such as the difficulty in creating a rigid boundary condition, measuring rotations or of extracting accurate residual terms from measurements. All of these issues compound dramatically as the number of connection points increases.

One alternative that is preferable from an experimental standpoint is to attach masses to the interface of the test article in order to exercise the interface and to bring a larger number of modes into the testable range. This approach seems to have been first explored in detail by Goldenberg and Shapiro [19]. About a decade later, Kanda, Wei, Allemang and Brown applied this method successfully to a few frame structures [20, 21], instrumenting the rigid masses to estimate their three translational and three rotational degrees of freedom and then removing their effect from the model. Chandler and Tinker studied the feasibility of this method analytically for two satellite systems, reporting very promising results [22]. Carne, Nelson and Dohrmann have also used this approach quite extensively to remove four distinct, rigid masses from a substructure [5, 23]. However, some difficulties have been encountered in other works [7, 8, 24]. First, it can be difficult to design a fixture that is massive enough to have the desired mass-loading effect while also being rigid in the frequency band of interest. This difficulty is compounded by the fact that the fixture must also be large relative to the wavelengths of the structure near the connection point so that one can accurately determine the rotation at that point [7]. When structures are connected at many points, this approach may not improve the substructure's modal basis much, as shown by Baker [8, 24], and one may require an excessive number of sensors since one must have at least six sensors per connection point to determine all of the displacements and rotations.

When masses are used to load an interface experimentally, their effect on the substructure must be removed prior to predicting the response of the built up structure. The process of removing one substructure from another is called substructure uncoupling or substructure de-coupling [25]. Substructure uncoupling also been studied by a few researchers, although the literature is somewhat sparse. A number of researchers have used substructure uncoupling to remove rigid masses from a structure [5, 20, 21, 23, 26], and a few have also accounted for the static flexibility in the joint between a fixture and the substructure in order to approximate the residual effect of out of band modes. A few works have removed a flexible substructure from a master system using frequency based substructuring. For example, Dong and McConnell [27] used FBS to infer connection point rotations using an instrumented, flexible fixture. Mottershead et al. [7, 8] developed a multi-input-multi-output FRF estimator that uses an FE model of the

fixture to estimate the uncoupled FRFs directly from measurements on the fixture, based on FBS theory. Ind and Ewins also studied the uncoupling problem to infer the dynamical properties of a delicate component from measurements remote to that component [28]. The works by Mottershead et al. and Dong & McConnell showed that good results could be obtained with appropriate care, although high sensitivity to noise seemed to be unavoidable in some circumstances. Ind [28] abandoned the FBS approach in favor of a model updating approach, citing high sensitivity to measurement errors as a major reason. Very recently, a few researchers have presented significant progress in this area. Sjovall and Abrahamsson studied the uncoupling problem using an FBS approach, showing that uncoupling predictions can be very sensitive to what they termed "generalized anti-resonances," or resonances of the substructure when all of the interface degrees of freedom are constrained. They presented a frequency-based substructuring method in [29] that utilizes responses away from the connection point to address this sensitivity, showing good results for both experimental and analytical measurements. D'Ambrogio and Fregolent also explored the use of responses away from the connection point in FBS uncoupling in [25].

This work builds upon those in a few ways. First, a methodology is presented that removes the effect of a fixture in the modal domain rather than using frequency responses as done in [25, 28, 29]. This greatly simplifies the data manipulation required and makes the results easier to interpret and store. This same approach could, in principle, be used to remove any linear dynamic system with mass, stiffness and damping, from another. The theory for doing so is presented and some of the consequences are elaborated. As in the prior works, the examples presented here show that erroneous predictions can be obtained unless measurements away from the connection point are utilized in the uncoupling procedure. However, the method presented in this work utilizes an over-determined set of measurements to enforce the removal of the subcomponent in a weak sense, which seems to reduce the sensitivity to measurement errors. The method is based on the modal filter concept [30] and is called Modal Constraints for Fixture and Subsystem (MCFS) or simply modal constraints. The method is applied to a substructuring problem involving the removal and coupling of two substructures with eight connection points, revealing that the interface can be adequately captured using only 36 sensors whereas the conventional approach would require at least 48 (three rotations and three displacements for each connection point). The approach presented here avoids the need to estimate the displacements and rotations at each connection point and the inaccuracies that this can introduce. The modal model obtained for each experimental subcomponent is coupled to an analytical model for the rest of the

structure and the procedure is shown to accurately predict the dynamics of the built up system over a significant frequency range.

The paper is organized as follows. Section 2.1 reviews modal substructuring theory as well as a few additional concepts that are important for the problems considered here. The extension to substructure uncoupling is presented in Section 2.2, with the conventional approach to treating constraints in Section 2.2.1, and the new modal constraint approach discussed in Section 2.2.2. The methods are applied to two systems in Section 3, a two-dimensional problem joining two beams after removing a fixture that mass-loads the experimental substructure, and a three dimensional problem in which a cylindrical structure is joined to a cap structure. Conclusions are presented in Section 4.

2. Theoretical Development

2.1. Review of Modal Substructure Coupling Theory

This section briefly reviews modal substructuring or Component Mode Synthesis (CMS) theory, following the notation in [12]. The reader is referred to [9, 12, 13, 31] for further details. We presume that the modal parameters for a number of subsystems have been derived either analytically or experimentally (see, e.g. [32, 33] for information on how to obtain these experimentally). In either case, one can use the modal parameters to construct the familiar second order, linear equations of motion for each subsystem. For example, denoting the first subsystem as A, one has.

$$\begin{aligned} \mathbf{I}\ddot{\mathbf{q}}_{\mathrm{A}} + \left[\,\backslash 2\zeta_r\omega_{r\backslash}\right]_{\mathrm{A}}\dot{\mathbf{q}}_{\mathrm{A}} + \left[\,\backslash \omega_r^{\,2}\,\backslash\right]_{\mathrm{A}}\mathbf{q}_{\mathrm{A}} &= \boldsymbol{\Phi}_{\mathrm{A}}{}^{T}\mathbf{F}_{\mathrm{A}} \\ \mathbf{y}_{\mathrm{A}} &= \boldsymbol{\Phi}_{\mathrm{A}}\mathbf{q}_{\mathrm{A}} \end{aligned} \quad (1),$$

where $\mathbf{I}$ denotes an $N\times N$ identity matrix, $\left[\,\backslash 2\zeta_r\omega_{r\backslash}\right]_{\mathrm{A}}$ an $N\times N$ diagonal matrix of modal damping constants, and $\left[\,\backslash \omega_r^{\,2}\,\backslash\right]_{\mathrm{A}}$ an $N\times N$ diagonal matrix of modal natural frequencies squared. This description assumes that the mode shape matrix, $\boldsymbol{\Phi}_{\mathrm{A}}$, is mass normalized and that reciprocity holds. The size of the mode shape matrix is $N_p\times N$, where N_p is the number of physical coordinates $\mathbf{y}_{\mathrm{A}}$, which is generally different than the number of modal degrees of freedom N. The vector $\mathbf{F}_{\mathrm{A}}$ contains the point forces and/or moments applied at the physical coordinates $\mathbf{y}_{\mathrm{A}}$. One could write the equations of motion for any additional subsystems (herein denoted B, C, …) in the same manner.

It is important to note that in some cases it might be convenient to describe the subcomponents in terms of their physical coordinates with physical mass, damping and stiffness matrices, **M**, **C** and **K** respectively as follows,

$$\mathbf{M}\ddot{\mathbf{y}}_A + \mathbf{C}\dot{\mathbf{y}}_A + \mathbf{K}\mathbf{y}_A = \mathbf{F} \tag{2},$$

although this view requires that the number of physical coordinates be equal to the number of modes or complications arise. In this work modal models are used exclusively, so the following development focuses on the modal description. However, it would be straightforward to use physical mass, damping and stiffness matrices in place of the diagonal matrices of modal parameters used here, and some possible reasons for doing so are highlighted later. One could also augment either of the representations in eqs (1) or (2) to include the residual flexibility of the truncated modes [17, 18], although those terms can be difficult to measure experimentally.

Subsystems described by the form in Eq. (1) can be joined by concatenating their modal coordinates, and then defining the appropriate constraints between them. For example, in order to join two subsystems, denoted A and B, which are described by their free modes, the concatenated equations are the following

$$\begin{bmatrix} \mathbf{I}_A & 0 \\ 0 & \mathbf{I}_B \end{bmatrix} \begin{Bmatrix} \ddot{\mathbf{q}}_A \\ \ddot{\mathbf{q}}_B \end{Bmatrix} + \begin{bmatrix} \left[2\zeta_r \omega_r \right]_A & \mathbf{0} \\ \mathbf{0} & \left[2\zeta_r \omega_r \right]_B \end{bmatrix} \begin{Bmatrix} \dot{\mathbf{q}}_A \\ \dot{\mathbf{q}}_B \end{Bmatrix} + \begin{bmatrix} \left[\omega_r^2 \right]_A & \mathbf{0} \\ \mathbf{0} & \left[\omega_r^2 \right]_B \end{bmatrix} \begin{Bmatrix} \mathbf{q}_A \\ \mathbf{q}_B \end{Bmatrix} =$$
$$= \begin{bmatrix} \mathbf{\Phi}_A^T & \mathbf{0} \\ \mathbf{0} & \mathbf{\Phi}_B^T \end{bmatrix} \begin{Bmatrix} \mathbf{F}_A \\ \mathbf{F}_B \end{Bmatrix} \tag{3},$$
$$\begin{Bmatrix} \mathbf{y}_A \\ \mathbf{y}_B \end{Bmatrix} = \begin{bmatrix} \mathbf{\Phi}_A & \mathbf{0} \\ \mathbf{0} & \mathbf{\Phi}_B \end{bmatrix} \begin{Bmatrix} \mathbf{q}_A \\ \mathbf{q}_B \end{Bmatrix}$$

where **0** denotes a matrix of zeros of the appropriate dimensions. We shall denote the number of modes in systems A and B as N_A and N_B respectively, and the number of physical coordinates N_{pA} and N_{pB}. This substructuring approach is easily generalized to many subsystems, as shown in [9, 12], or one could treat a general problem by repeatedly applying the approach outlined above to pairs of systems.

Linear constraints between the substructures can be written as,

$$\mathbf{a}_p \begin{Bmatrix} \mathbf{y}_A \\ \mathbf{y}_B \end{Bmatrix} = \mathbf{0} \tag{4}$$

(e.g. $\mathbf{a}_p$ = [-1, 1] for the case where $\mathbf{y}_A$ and $\mathbf{y}_B$ are scalars and one wishes to apply the scalar constraint $\mathbf{y}_A$=$\mathbf{y}_B$). The number of rows in $\mathbf{a}_p$ is equal to the number of constraints, denoted N_{ce}. Substituting from Eq. (3) one obtains the constraints between the total set of generalized coordinates $\{\mathbf{q}_A^T, \mathbf{q}_B^T\}^T$,

$$\mathbf{a}\begin{Bmatrix}\mathbf{q}_A\\ \mathbf{q}_B\end{Bmatrix}=\mathbf{0} \tag{5}$$

where

$$\mathbf{a}=\mathbf{a}_p\begin{bmatrix}\boldsymbol{\Phi}_A & \mathbf{0}\\ \mathbf{0} & \boldsymbol{\Phi}_B\end{bmatrix}. \tag{6}$$

The constraint equations are used to solve for some of the generalized coordinates in terms of the others [12]. It should be noted here that the perfect compatibility required by Eq. (4) can lead to excessive stiffening if there are multiple connection points. This issue will be addressed in Section 2.2.2. Using the method presented in [9], one uses the constraints to find a transformation that obtains the full coordinate vector from a set of unconstrained generalized coordinates, $\mathbf{x}_u$, as follows.

$$\begin{Bmatrix}\mathbf{q}_A\\ \mathbf{q}_B\end{Bmatrix}=\mathbf{B}\mathbf{x}_u \tag{7}$$

Substituting this relationship into Eq. (5), one finds that $\mathbf{B}$ must satisfy

$$\mathbf{a}\mathbf{B}\mathbf{x}_u=\mathbf{0}, \tag{8}$$

so, $\mathbf{B}$ can be any matrix that resides in the null space of $\mathbf{a}$ [9].

$$\mathbf{B}=null\left(\mathbf{a}\right) \tag{9}$$

The constraint matrix, $\mathbf{a}$, which has dimension N_{ce} by (N_B + N_A) should have maximal rank, otherwise some of the constraints are ineffectual.

After substituting Eq. (7) into Eq. (2), the equations of motion become the following.

$$
\begin{aligned}
\hat{\mathbf{M}}\ddot{\mathbf{x}}_u + \hat{\mathbf{C}}\dot{\mathbf{x}}_u + \hat{\mathbf{K}}\mathbf{x}_u &= \mathbf{Q} \\
\hat{\mathbf{M}} &= \mathbf{B}^T \begin{bmatrix} \mathbf{I}_A & \mathbf{0} \\ \mathbf{0} & \mathbf{I}_B \end{bmatrix} \mathbf{B} \\
\hat{\mathbf{C}} &= \mathbf{B}^T \begin{bmatrix} \left[\backslash 2\zeta_r \omega_r \backslash \right]_A & \mathbf{0} \\ \mathbf{0} & \left[\backslash 2\zeta_r \omega_r \backslash \right]_B \end{bmatrix} \mathbf{B} \\
\hat{\mathbf{K}} &= \mathbf{B}^T \begin{bmatrix} \left[\backslash \omega_r^2 \backslash \right]_A & \mathbf{0} \\ \mathbf{0} & \left[\backslash \omega_r^2 \backslash \right]_B \end{bmatrix} \mathbf{B} \\
\begin{Bmatrix} \mathbf{y}_A \\ \mathbf{y}_B \end{Bmatrix} &= \begin{bmatrix} \mathbf{\Phi}_A & \mathbf{0} \\ \mathbf{0} & \mathbf{\Phi}_B \end{bmatrix} \mathbf{B}\mathbf{x}_u
\end{aligned}
\tag{10}
$$

If N_{ce} constraint equations are enforced, then the coupled system will have only $N_B + N_A - N_{ce}$ degrees of freedom. However, all of the physical coordinates $\mathbf{y}$ for any of the subsystems are always available in the system model, even after enforcing a constraint, although some of them may be equal or nearly equal to one another due to the constraint (i.e. one can find $\mathbf{q}_A$ or $\mathbf{q}_B$ using Eq. (7) and then use Eq. (3) to find $\mathbf{y}_A$ and $\mathbf{y}_B$, no matter what constraints have been employed). One will also typically desire to compute the modes of the coupled system by finding the eigenvalue decomposition of $\hat{\mathbf{K}}$, $\hat{\mathbf{M}}$ (or of $\hat{\mathbf{K}}$, $\hat{\mathbf{C}}$, $\hat{\mathbf{M}}$ if state space modes are of interest). The last of Eqs. (10) shows that the displacement, and hence the modes of the assembled structure are comprised of linear combinations of the modes of the individual subsystems. All of the operations described above have been automated and are implemented in a Matlab® function, dubbed “ritzscomb”, which is freely available on the Matlab® Central File Exchange.

2.2. Method for Removing Fixture Effects from an Experimental Model

One can also use the substructuring method above to remove a fixture from an assembly. To better understand the approach, it is helpful to consider the simple spring-mass problem shown in Figure 1.

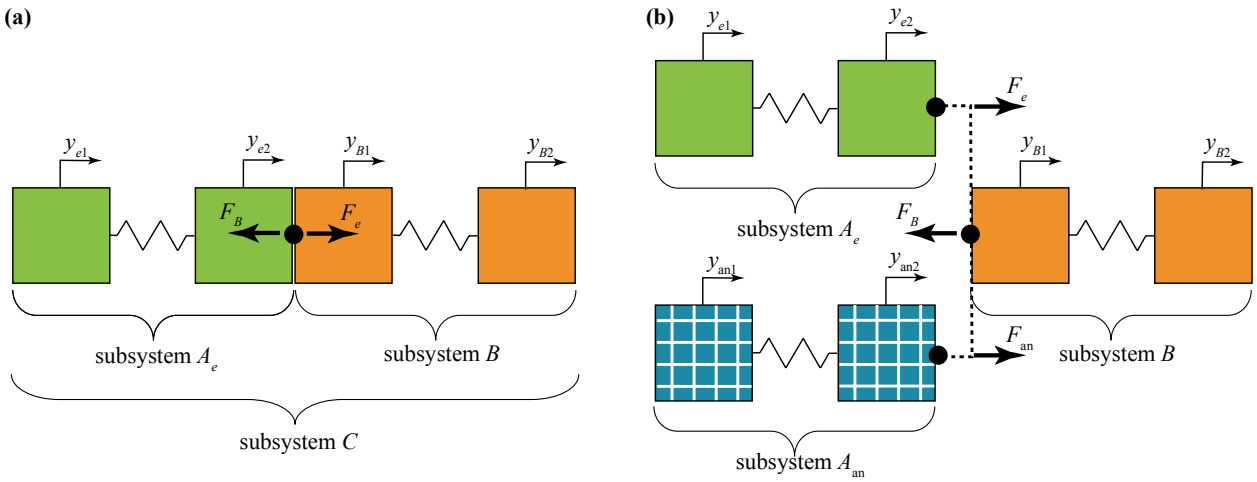

Figure 1: Basic substructure uncoupling problem. (a) Experimental subsystem C (left) is comprised of subsystems A_e and B. The forces that each subsystem exerts on the other in the assembly are denoted F_e and F_B respectively. (b) An analytical model of A_e, denoted A_{an}, is joined to C at the connection point (the points connected by the dashed line all have the same motion).

We desire to remove the effect of the two left-most masses from the experimental system C in order to estimate the equations of motion of system B. System A exists as experimental hardware connected to C, and its (unknown) system parameters and modal coordinates are denoted *e*. In this configuration the constraint force between the subsystems is $\mathbf{F}_B = \mathbf{F}_e$. (i.e. system A_e exerts an unknown force $\mathbf{F}_e$ on system B such that the two to have the same motion at the connection point.) To cancel the interface force and remove the effect of subsystem A_e, an analytical model of A is constructed, denoted A_{an}, and connected to system C at the connection point between A and B. The modal parameters of the model are known and both those and the force at the interface are denoted with subscripts "an" (masses with grid shading). The net force on system B is now $\mathbf{F}_B = \mathbf{F}_e + \mathbf{F}_{an}$ and so the effect of the fixture is effectively removed if the forces from the analytical model, "an", cancel those from the actual hardware, *e*, so that $\mathbf{F}_e + \mathbf{F}_{an} = 0$. The equations of motion for "an" and *e* can be used to write the interface forces, which are given below for a general problem.

$$\mathbf{I}_e \ddot{\mathbf{q}}_e + \left[2\zeta_r \omega_r \right]_e \dot{\mathbf{q}}_e + \left[\omega_r^2 \right]_e \mathbf{q}_e = \boldsymbol{\Phi}_e{}^{\mathrm{T}} \mathbf{F}_e \tag{11}$$

$$\mathbf{I}_{an} \ddot{\mathbf{q}}_{an} + \left[2\zeta_r \omega_r \right]_{an} \dot{\mathbf{q}}_{an} + \left[\omega_r^2 \right]_{an} \mathbf{q}_{an} = \boldsymbol{\Phi}_{an}{}^{\mathrm{T}} \mathbf{F}_{an} \tag{12}$$

Note that in practice the modal parameters of A_e are not precisely known, nor is the force $\mathbf{F}_e$, since this system represents actual hardware, but this discussion is still helpful in revealing the condition under which the effects of A_e can be removed. Adding these two equations one obtains,

$$\mathbf{I}_e\ddot{\mathbf{q}}_e + \mathbf{I}_{\text{an}}\ddot{\mathbf{q}}_{\text{an}} + \left[\backslash 2\zeta_r\omega_{r\backslash}\right]_e \dot{\mathbf{q}}_e + \left[\backslash 2\zeta_r\omega_{r\backslash}\right]_{\text{an}} \dot{\mathbf{q}}_{\text{an}} + \left[\backslash \omega_{r\backslash}^2\right]_e \mathbf{q}_e + \left[\backslash \omega_{r\backslash}^2\right]_{\text{an}} \mathbf{q}_{\text{an}} = \\ = \mathbf{\Phi}_e{}^{\text{T}}\mathbf{F}_e + \mathbf{\Phi}_{\text{an}}{}^{\text{T}}\mathbf{F}_{\text{an}} \tag{13}$$

so the interface forces can be made to cancel if the following conditions are satisfied.

1.) The modal parameters of the analytical and true fixtures are equal and opposite, i.e. $\left[\backslash \omega_{r\backslash}^2\right]_{\text{an}} = -\left[\backslash \omega_{r\backslash}^2\right]_e$ and similarly for the mass and damping terms.

2.) The motion of both the experimental and analytical fixtures is the same, $\{\mathbf{q}_{\text{an}}(t)\} = \{\mathbf{q}_e(t)\}$

3.) The mode shapes of both the experimental and analytical models are equal $\mathbf{\Phi}_{\text{an}} = \mathbf{\Phi}_e$.

4.) The interface force vector is in the range space of $\mathbf{\Phi}_{\text{an}}{}^{\text{T}}$.

If all of these conditions are satisfied, then one can simplify Eq. (13) to show that $\mathbf{F}_{\text{an}} + \mathbf{F}_e = \mathbf{0}$, so the net force on substructure B by the fixtures is zero. For the example problem shown in Figure 1 the interface force is a scalar applied to the second mass and the analytical and experimental subsystems each contain 2 degrees-of-freedom, so one obtains $\{0 \quad F_{\text{an}}\}^{\text{T}} + \{0 \quad F_e\}^{\text{T}} = \{0 \quad 0\}^{\text{T}}$. However, if any of the conditions are violated then there will be a non-zero force at the connection point. For example, suppose that all of the conditions are satisfied except that the analytical system matrices, $\left[\backslash \omega_{r\backslash}^2\right]_{\text{an}}$ and $\left[\backslash 2\zeta_r\omega_{r\backslash}\right]_{\text{an}}$, while opposite of the experimental ones, are not precisely equal and opposite (condition 1). This situation commonly arises since the analytical model is an approximation of the experimental fixture. In this case the interface force becomes

$$\mathbf{q}_e = \mathbf{q}_{\text{an}} \\ [\mathbf{0}]\ddot{\mathbf{q}}_e + \left[\left[\backslash 2\zeta_r\omega_{r\backslash}\right]_e - \left[\backslash 2\zeta_r\omega_{r\backslash}\right]_{\text{an}}\right]\dot{\mathbf{q}}_{\text{e}} + \left[\left[\backslash \omega_{r\backslash}^2\right]_e - \left[\backslash \omega_{r\backslash}^2\right]_{\text{an}}\right]\mathbf{q}_{\text{e}} = \\ = \mathbf{\Phi}_e{}^{\text{T}}\left(\mathbf{F}_e + \mathbf{F}_{\text{an}}\right) \tag{14}$$

This could clearly give rise to a non-zero interface force. Those interface forces would behave like stiffness and mass terms, reflecting effects of the fixture that have not been completely removed. An even more problematic case can arise if the motion of the analytical and experimental fixtures is not precisely the same.

At this juncture, it is worth noting that the 4th condition might not be necessary for every problem. If it is not satisfied then the interface forces cancel only in a weak sense. The specifics of the problem will dictate whether this is adequate.

In all of the above the interface forces have been introduced merely to justify the procedure. The interface forces do not enter in to the actual operations required to implement this uncoupling methodology. For the example illustrated in Figure 1 the operations are as follows. The equations of motion for A_{an} and C are concatenated, as was done in Eq. (3), only now we make the diagonal mass, damping and stiffness matrices for subsystem A_{an} negative to remove A_{an}'s effects from C.

$$\begin{bmatrix} -\mathbf{I}_{A_{an}} & 0 \\ 0 & \mathbf{I}_C \end{bmatrix} \begin{Bmatrix} \ddot{\mathbf{q}}_{A_{an}} \\ \ddot{\mathbf{q}}_C \end{Bmatrix} + \begin{bmatrix} -\left[\backslash 2\zeta_r \omega_r \backslash \right]_{A_{an}} & \mathbf{0} \\ \mathbf{0} & \left[\backslash 2\zeta_r \omega_r \backslash \right]_C \end{bmatrix} \begin{Bmatrix} \dot{\mathbf{q}}_{A_{an}} \\ \dot{\mathbf{q}}_C \end{Bmatrix} + \begin{bmatrix} -\left[\backslash \omega_r^2 \backslash \right]_{A_{an}} & \mathbf{0} \\ \mathbf{0} & \left[\backslash \omega_r^2 \backslash \right]_C \end{bmatrix} \begin{Bmatrix} \mathbf{q}_{A_{an}} \\ \mathbf{q}_C \end{Bmatrix} = \begin{bmatrix} \mathbf{\Phi}_{A_{an}}{}^T & \mathbf{0} \\ \mathbf{0} & \mathbf{\Phi}_C{}^T \end{bmatrix} \begin{Bmatrix} \mathbf{F}_{A_{an}} \\ \mathbf{F}_C \end{Bmatrix} \tag{15}$$

One can then use the same procedure outlined in Eq. (4) through (10) to apply constraints between A_{an} and C. The results depend on how A_{an} and C are constrained, as will be described in the following two subsections. Two approaches are described, the first of which is a straightforward extension of the traditional approach, here called the connection point method. A new approach is presented in Section 2.2.2 that involves constraining the modal degrees of freedom of the fixtures. This new approach is dubbed Modal Constraints for Fixture and Subsystem (MCFS), or simply "modal constraints". When these methods are applied experimentally, more robust results are obtained using the latter. That approach also offers new freedom when joining substructures at multiple points, as illustrated in Section 3.2.

2.2.1. Connection Point Constraints (CPT)

Previous works that have employed mass-loaded interface modes [20, 21, 24] have combined the (negative) models of the rigid masses to the experimental substructures at the points at which they meet physically using the following constraints. The subscript "an" on A is dropped from here forward to simplify the notation.

$$\mathbf{y}_{C,CPT} = \mathbf{y}_{A,CPT} \tag{16}$$

Here this will be referred to as the Connection PoinT (CPT) method and the subset of physical degrees of freedom on system A and C that correspond to the connection are denoted with the subscript CPT. This leads to a signed Boolean constraint matrix $\mathbf{a}_p$ in Eq. (4).

In practice the connection point motion of system C usually is not measured, so measurements are taken at discrete points on the attached fixture and used to infer the connection point motion. In the past, it has been

assumed that the mass moves as a rigid body (see, e.g. [20, 21]). Denoting the measureable points on the fixture with the subscript *m*, the motion of the fixture was assumed to be a linear combination of the rigid body mode shapes of the fixture $\mathbf{\Phi}_{\mathrm{A}}$, so it could be written as follows

$$\begin{Bmatrix} \mathbf{y}_{\mathrm{C,CPT}} \\ \mathbf{y}_{\mathrm{C},m} \end{Bmatrix} = \begin{bmatrix} \mathbf{\Phi}_{\mathrm{A,CPT}} \\ \mathbf{\Phi}_{\mathrm{A},m} \end{bmatrix} \mathbf{q}_{\mathrm{A}} \tag{17}$$

where the upper and lower partitions are the rigid body mode shapes at the connection (CPT) and measurement points (*m*) respectively. The mode shapes of the fixture are estimated using an analytical model of the fixture. Assuming that the mode shapes are linearly independent on the measurement point set, and that there are at least as many measurement points as there are rigid body modes, then the connection point motion of system C is found by solving the lower partition for $\mathbf{q}_{\mathrm{A}}$ and substituting into the upper partition, resulting in the following observation equation,

$$\mathbf{y}_{\mathrm{C,CPT}} = \mathbf{\Phi}_{\mathrm{A,CPT}} \mathbf{\Phi}_{\mathrm{A},m}{}^{\dagger} \mathbf{y}_{\mathrm{C},m} \tag{18}$$

where $[\ ]^{\dagger}$ denotes the Moore-Penrose pseudo-inverse or an overdetermined least-squares solution. This can be viewed as a modal test-analysis model for the fixture [34], or as a particular case of sensor set expansion using a certain finite element model. A similar approach was used to find the motion at an unmeasured point in [20, 21, 35-37].

This expression can be substituted into Eq. (16) and rearranged into the form in Eq. (4). The preceding development can readily be extended for a fixture that is flexible by augmenting the modal description in Eq. (17) to also include the free-elastic mode shapes of the fixture. In that case, Eq. (18) constitutes a modal filter [30] that estimates the modal motion of the fixture and then uses the connection point mode shapes to estimate the connection point motion.

This substructure coupling approach will succeed only if the connection point motion can accurately be estimated from the motion at the measurement points. Balmès discussed a number of approaches in [38] showing that grave errors can be incurred if either the test results or the FEM model are not accurate. Some of these difficulties stem from the fact that the analytical and experimental fixtures are required to have the same motion only at the connection point. Returning to the example in Figure 1, a constraint that imposes equal motion at the

connection point, i.e. $\mathbf{y}_{e,2} = \mathbf{y}_{\text{an},2}$ does not force $\mathbf{y}_{e,1}$ and $\mathbf{y}_{\text{an},1}$ to have the same motion. Those degrees of freedom will only have the same motion if the parameters of each system are equal and if the connection point(s) render the system controllable. When those conditions are met, the motion enforced at the connection point causes the same response for each subsystem and the fixtures exert zero net force on subsystem B. On the other hand, if the fixture and its negative model differ due to model inaccuracy or small errors in the test, then their states will not be equal at all times and the fixtures will exert a spurious force on subsystem B. This phenomenon is observed in the examples that follow in Section 3, so the MCFS approach was created (described in the following subsection) in order to address it.

2.2.2. Modal Constraints for Fixture and Subsystem (MCFS)

Another way to assure that the two fixtures A_{an} and A_e undergo the same motion is to constrain them at a set of points that are distributed spatially, which are here referred to as the measurement points and denoted with subscript *m*.

$$\mathbf{y}_{\text{C},m} = \mathbf{y}_{\text{A},m} \tag{19}$$

However, some of the constraints above are redundant if the fixture model has fewer modes than there are measurement points, N_M. There will also inevitably be small test errors in each of the responses. These errors may cause locking of the two systems resulting in wildly erroneous predictions. One would prefer that Eq. (19) instead be satisfied in a least squares sense so that measurement errors do not contaminate the constraints. The Modal Constraints for Fixture and Subsystem (MCFS) method seeks to do exactly this, using the following weighted form of the constraints above,

$$\mathbf{\Phi}_{\text{A},m}{}^{\dagger}\mathbf{y}_{\text{C},m} = \mathbf{\Phi}_{\text{A},m}{}^{\dagger}\mathbf{y}_{\text{A},m} \tag{20}$$

where the subscript *A* denotes that we are using the mode matrix for fixture A to form the constraints. The right hand side is equal to the modal coordinates of the fixture, $\mathbf{q}_{\text{A}}$, so physically, Eq. (20) constrains the modal coordinates of the fixture (system A) to their orthogonal projection onto the C system's motion. Using this approach there is one constraint equation for each mode that is included in $\mathbf{\Phi}_{\text{A},m}$. One typically has more sensors than modes, so there are fewer constraints than there are sensors, so this approach does not enforce strictly equal the displacement between the measurement points $\mathbf{y}_{\text{C},m}$ and $\mathbf{y}_{\text{A},m}$. In contrast, when the CPT method is used the

motion at the connection point is forced to be precisely equal and there is one constraint for each connection point degree of freedom no matter how many modal degrees of freedom the structure has.

2.2.3. Fixture Design

Based on the theory presented above and reviewed in Section 2.1, the following guidelines have been developed for fixture design.

1. One should design the fixture so that it can be instrumented to capture all of its relevant dynamic modes so that $\boldsymbol{\Phi}_{\mathrm{A},m}$ will be well conditioned for inversion in Eq. (20).
2. When the fixture is attached to the test article, the experimental system should have an adequate number of modes in the testable bandwidth. The mass of the fixture can be chosen to bring more modes down into the testable bandwidth.
3. Avoid fixture designs that contain joints, intricate geometry, or other features that are difficult to accurately model analytically, as these will lead to mismatch between the experimental and analytical fixtures causing errors in the subtraction. The fixture should be easy to model so that it accurately predicts the fixture dynamics without a significant fixture model correlation effort. Making the fixture of one piece, without any joints, goes a long way toward meeting this guideline.
4. The joint between the fixture and the test article should replicate the actual joint in the system of interest as closely as possible, to capture the joint stiffness and damping.
5. The fixture's impedance should roughly resemble that of the built-up structure. One strategy is to design a fixture to locally mimic the stiffness and mass of the other substructure to which the experimental substructure will be connected. The fixture might just be a chopped off version of the other substructure which precisely mimics the mass and stiffness near the connection interface.

Also, it is usually convenient if the fixture's modes are well spaced, so they can be easily extracted from measurements. One key consideration is the number of dynamic modes to include in $\boldsymbol{\Phi}_{\mathrm{A},m}$. For simple fixtures, such as that used in Section 3.1, one can fairly easily estimate the number of dynamic modes of the fixture that are likely to reside in or near the frequency band of interest. In other cases this may be challenging, but one can always assess this after measurements are taken by reconstructing the measured mode shapes of system C on the fixture's modal basis and comparing that reconstruction with the actual measurements. This was done in [23] for an FBS procedure and was found to serve as a valuable error check during the experiment.

3. Applications

3.1. Beam System

A simple structure was designed to evaluate the CMS procedures, which is comprised of two beams as depicted in Fig. 2. The goal of the substructuring procedure is to correctly determine the frequency response functions of system E between points 1 and 2 at the ends of beam E. Beam B, which is 30.5 cm long, is the substructure whose model will be derived from test. Fixture A_e (11.7 cm tall) is attached to beam B during the tests at the connection point y_c forming substructure C, the system that is actually tested. The connection point motion is not measured during the test. Six accelerometers are placed on Fixture A_e to characterize its motion as shown in Figure 3. An analytical model of Fixture A was developed using Timoshenko beam elements, denoted A_{an}, and which will be used to remove the fixture's effects from System C. The 61 cm beam D was modeled analytically using Euler-Bernoulli theory, although its natural frequencies were adjusted to more closely match the frequencies of a real beam of the same dimensions. All of the components are made of steel. Beams B and D are 1.9 cm high by 2.54 cm wide; Fixture A's cross section is 2.54 cm square. The figure below illustrates the coupling/uncoupling process.

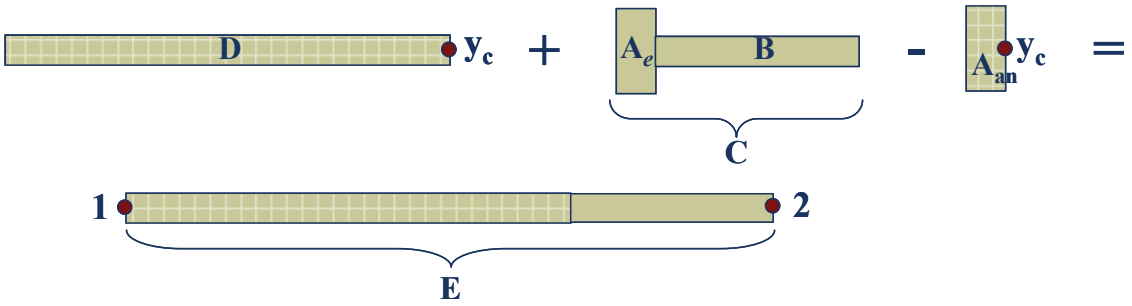

Figure 2: Experimental-Analytical substructuring problem consisting of two beams. An experimental model for beam B is to be joined to an analytical beam D after fixture A_e is removed using CMS uncoupling.

Leaving out the damping terms for the sake of clarity, the uncoupled equations of motion in the form of Eq. (3) for this example are

$$\begin{bmatrix} -\mathbf{I}_{A_{an}} & \mathbf{0} & \mathbf{0} \\ \mathbf{0} & \mathbf{I}_C & \mathbf{0} \\ \mathbf{0} & \mathbf{0} & \mathbf{I}_D \end{bmatrix} \begin{Bmatrix} \ddot{\mathbf{q}}_{A_{an}} \\ \ddot{\mathbf{q}}_C \\ \ddot{\mathbf{q}}_D \end{Bmatrix} + \begin{bmatrix} -\left[\omega_r^2\right]_{A_{an}} & \mathbf{0} & \mathbf{0} \\ \mathbf{0} & \left[\omega_r^2\right]_C & \mathbf{0} \\ \mathbf{0} & \mathbf{0} & \left[\omega_r^2\right]_D \end{bmatrix} \begin{Bmatrix} \mathbf{q}_{A_{an}} \\ \mathbf{q}_C \\ \mathbf{q}_D \end{Bmatrix} = \begin{bmatrix} \mathbf{\Phi}_{A_{an}}^T & \mathbf{0} & \mathbf{0} \\ \mathbf{0} & \mathbf{\Phi}_C^T & \mathbf{0} \\ \mathbf{0} & \mathbf{0} & \mathbf{\Phi}_D^T \end{bmatrix} \begin{Bmatrix} \mathbf{F}_{A_{an}} \\ \mathbf{F}_C \\ \mathbf{F}_D \end{Bmatrix} \tag{21}$$

Two cases are considered. In the first, connection point constraints are used between A_e (a part of system C) and A_{an}. A modal filter was used to estimate the connection point motion and then the CPT method was used to

constrain the negative fixture model A_{an} to C so the constraint is $\boldsymbol{\Phi}_{A_{an},CPT}\mathbf{q}_{A_{an}} - \boldsymbol{\Phi}_{A_{an},CPT}\boldsymbol{\Phi}_{A_{an},m}{}^{\dagger}\mathbf{y}_{C,m} = 0$. Then, connection point constraints were again used to constrain A to D with the constraint $\boldsymbol{\Phi}_{A_{an},CPT}\mathbf{q}_{A_{an}} - \mathbf{y}_{D,CPT} = \mathbf{0}$. In terms of the modal coordinates of each of the subsystems, the constraints are

$$\begin{bmatrix} \boldsymbol{\Phi}_{A_{an},CPT} & -\boldsymbol{\Phi}_{A_{an},CPT}\boldsymbol{\Phi}_{A_{an},m}{}^{\dagger}\boldsymbol{\Phi}_{C,m} & \mathbf{0} \\ \boldsymbol{\Phi}_{A_{an},CPT} & \mathbf{0} & -\boldsymbol{\Phi}_{D,CPT} \end{bmatrix} \begin{Bmatrix} \mathbf{q}_{A_{an}} \\ \mathbf{q}_{C} \\ \mathbf{q}_{D} \end{Bmatrix} = \mathbf{0} \tag{22}$$

which is now in the form of Eq. (5). One can then use the procedure outlined in Section 2.1 to enforce these constraints and compute the modes of the coupled system.

For the second case, modal constraints were used to connect the analytical fixture A_{an} to C. The constraint between those two systems is then $\mathbf{q}_{A_{an}} - \boldsymbol{\Phi}_{A_{an},m}{}^{\dagger}\mathbf{y}_{C,m} = 0$. A_{an} and D are again connected at the connection point as was done above. At first it seems counter intuitive to connect D to A_{an} since we have just "removed" A from C, but recall that all of the physical coordinates are always valid even after a subcomponent has been removed. The total set of constraint equations for the MCFS case is then.

$$\begin{bmatrix} \mathbf{I} & -\boldsymbol{\Phi}_{A_{an},m}{}^{\dagger}\boldsymbol{\Phi}_{C,m} & \mathbf{0} \\ \boldsymbol{\Phi}_{A_{an},CPT} & \mathbf{0} & -\boldsymbol{\Phi}_{D,CPT} \end{bmatrix} \begin{Bmatrix} \mathbf{q}_{A_{an}} \\ \mathbf{q}_{C} \\ \mathbf{q}_{D} \end{Bmatrix} = \mathbf{0} \tag{23}$$

It is interesting to note that first row in the constraint matrix in Eq. (22) is identical to corresponding row in Eq. (23) except that the former is premultiplied by $\boldsymbol{\Phi}_{A_{an},CPT}$. The fixture is approximated with four modes, yet there are only three connection point degrees-of-freedom (translation in two directions and rotation), so $\boldsymbol{\Phi}_{A_{an},CPT}$ has four columns but only three rows. Hence, Eqs. (22) comprise one fewer constraint than do Eqs. (23).

It is well known that the free-modes of a beam are not an efficient basis for substructuring predictions [17, 18]. To determine whether mass-loading was important for this problem, a simple one-dimensional finite element model of the beams was used to simulate the substructuring process. The testable bandwidth was considered to be 6400 Hz for FE simulation. The FE model revealed that if one couples all of the free bending modes of beam B below 6400 Hz (three elastic modes) to the FE model for beam D, one obtains errors in the built-up system natural frequencies as large as 5% for some of the modes below 6400 Hz (due to modal truncation). On the other hand, if beam B is mass-

loaded with a rigid mass whose inertia properties are the same as Fixture A's, then one obtains four modes below 6400 Hz and the estimates for the coupled system natural frequencies are within 0.3% of the analytical values. Hence, the fixture has a very important mass loading effect for this system.

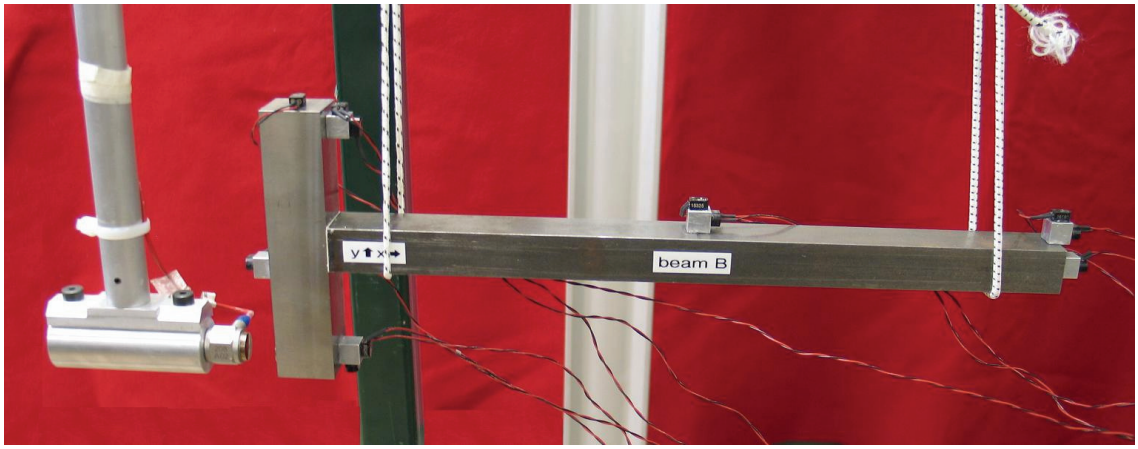

Figure 3: Photograph of experimental setup for testing system C using an impact hammer. System C is comprised of beam B and fixture A_e.

The actual hardware shown in Fig. 3 (system C) was tested using impact excitation. An impact hammer with a steel tip provided excitation at three points. Consistent alignment was assured by mounting the impact hammer on a bearing and carefully aligning the system before acquiring measurements. The fixture was attached to beam B using a single bolt with dental cement on the mating surfaces to reduce the nonlinearity of the joint. (Prior tests without dental cement revealed that the T-beam's response was somewhat nonlinear [39].) The excitation was adequate out to about 9000 Hz, below which six modes were extracted. These were supplemented with the analytically derived rigid body modes and used to create a modal model of the T-beam [15]. Three rigid body modes and one elastic bending mode were provided from the analytical fixture model. The measured modal damping ratios were used for the C system while the elastic modes of A_{an} and D were given modal damping ratios of 0.0008 and the rigid body modes were given zero damping. The substructuring procedure described previously was then used to couple these to estimate the modes, and from those the FRFs of Beam E.

Figure 4 shows the axial FRFs predicted between the measurement points 1 and 2 on the total structure (see Fig. 2) using the CPT and MCFS methods. An analytical prediction, tuned to match the modal properties of an actual 90.3 cm beam, is also shown as an indicator of truth. Both methods accurately predict the frequency and amplitude of the first axial mode, but the CPT method greatly underestimates the frequency of the second axial mode. Furthermore, the FRF from the CPT method has an antiresonance near 5800 Hz, which is not reasonable since it can

be shown that there are no antiresonances in the FRF of a beam whose output and excitation points are on opposite ends. The lateral FRFs found using the CPT and MCFS methods both agreed very closely with the analytical result, as shown in Fig. 5.

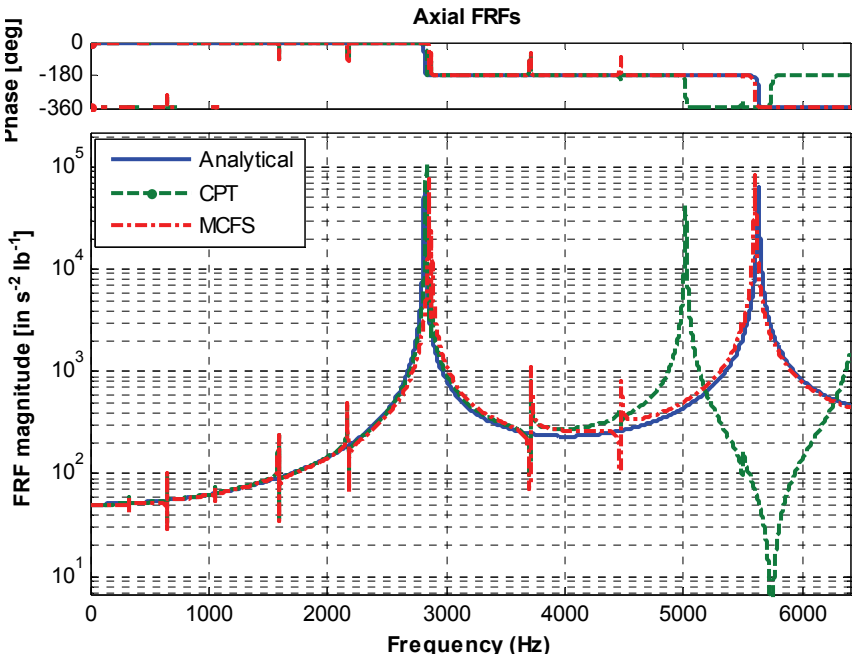

Figure 4: Axial FRFs between points 1 and 2 of beam E created using modal parameters obtained from substructuring predictions. Lines correspond to analytical result (solid), MCFS result (dash-dot) and CPT result (dash).

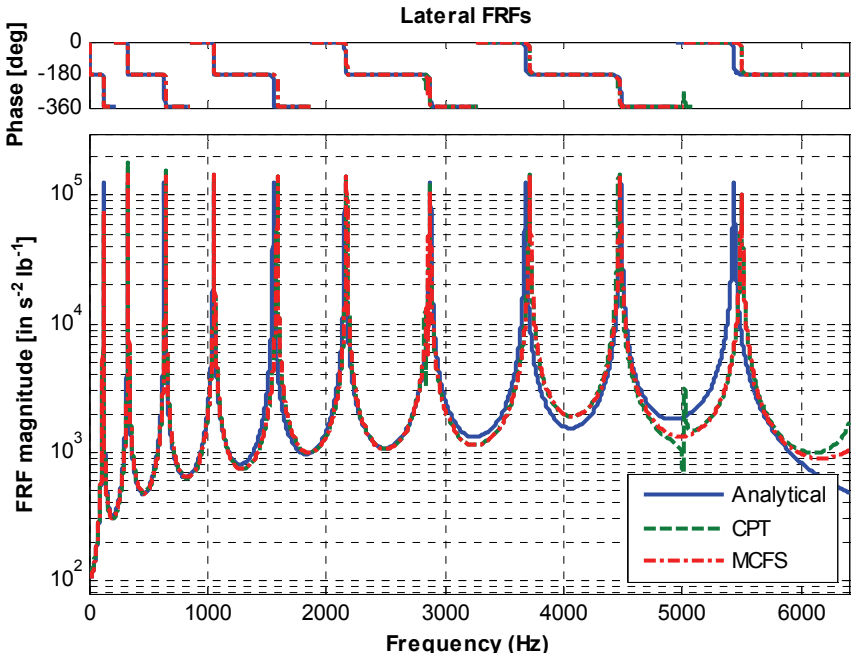

Figure 5: Lateral FRFs between points 1 and 2 of beam E derived from experimentally measured mode shapes for system C. Lines correspond to analytical result (solid), MCFS result (dash-dot) and CPT result (dash).

Various modifications to the fixture model were explored, and the experimental results were checked and re-checked, but none of these efforts improved the performance of the CPT method for the beam's second axial mode. However, when the CPT method was employed with a rigid fixture model the CPT method predicted two axial modes in the bandwidth of interest and didn't produce a spurious zero in the FRFs, but the predicted frequencies for both axial modes were about 700 Hz too low, presumably due to the fixture's neglected elasticity, as shown in our preliminary work [14].

As mentioned previously, one can evaluate the effectiveness of the constraint conditions by comparing the motion of the measurement points on both the experimental fixture and the negative fixture model for each of the modes of the combined system. This comparison is shown in Fig. 6 for the beam's first axial mode. Circles show the undeformed locations of the accelerometers shown in Fig. 3. The displaced mode shape of each accelerometer is also shown with triangles for the experimental fixture (part of the C system) and crosses for the analytical model of fixture, A_{an}. Note that uniaxial accelerometers were used, so each displacement is in a single direction only, as indicated by the letter in the node name for each sensor. The left-hand pane shows that when the MCFS method is used to join the subsystems, the motion of the A_{an} and C measurement points matches closely as desired, implying that the modal constraints have effectively enforced equivalent motion between the two systems. When the CPT

method is used as shown in the right hand pane, the motions differ considerably between A_{an} and C, indicating errors in the coupling. The difference between the mode shape at the A_{an} and C sensors was less than 0.4% of the maximum for the MCFS method while they were as large as 27% for the CPT method. For the second axial mode, the maximum percent differences over the measurement points were 4% and 141% respectively for the MCFS and CPT methods. The motion on the A and C systems matched very closely for all of the bending modes of the E system using either CPT or MCFS constraints, and this was also the case when the fixture's flexibility was ignored as shown in [14], suggesting that the fixture was essentially rigid for bending motions of system C.

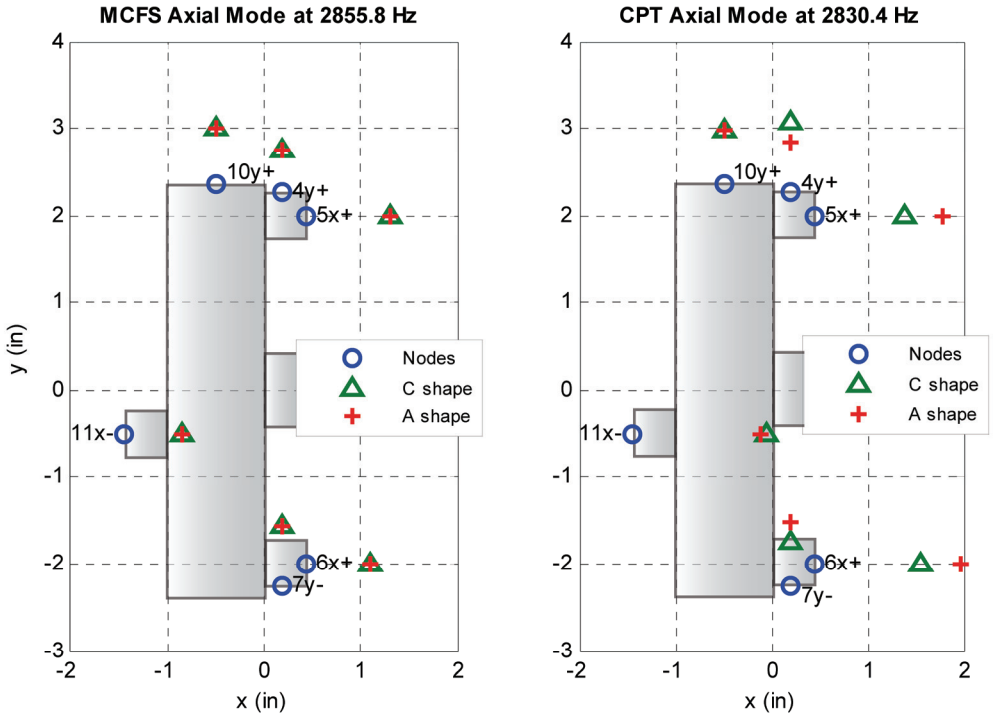

Figure 6: Mode shapes of 1st axial mode at the fixture's measurement points, found using MCFS and CPT methods to join the substructures. The mode shapes show that the A_{an} and C fixtures have nearly the same motion for the MCFS method, while significant difference are observed between the corresponding sensors when the CPT method is used.

Discussion:

These analyses may explain why the FRF predicted from the MCFS results is so much more accurate than the CPT result in Fig. 4, while both gave similar results for the bending FRFs in Fig. 5. The fact that the motion of the C and negative A_{an} systems differs when the CPT method is used perhaps explains the origin of the spurious zero in the CPT prediction in the axial direction, and the error in the CPT predicted 2nd axial natural frequency. On the other hand, both methods give good results for this system for the bending modes in the frequency band of interest.

It appears that this fixture's flexibility is really only important to the axial modes of the coupled system, which are more faithfully reproduced by the MCFS method.

One observes in Fig. 4, that both CPT and MCFS show spurious spikes at most of the bending mode frequencies, indicating that the substructuring predictions substantially overestimate the coupling between bending and axial motion. This is probably because the axial accelerometers register motion from bending modes simply due to their cross axis sensitivity (up to three percent for these accelerometers).

3.2. Cylindrical System

The second system considered consists of two substructures that are joined at multiple points. Whereas the fixture used on the beam would work if it was perfectly rigid, a flexible fixture was needed to capture the multiple point interface between the components in this assembly; a rigid fixture would eliminate important motion between the connection points. A schematic of this problem is shown in Fig. 7. The cylinder plus one copy of the attached fixture (subsystem A_{an}) in the upper-left comprise subsystem D, the part of this system that is modeled analytically. The experimental substructure C is shown in the upper-right, made up of a plate with a beam attached at its center (system B) and a fixture (system A_e) that has four tabs around its circumference. The tabs were designed into the fixture to add mass and to bring the bending and axial modes of the experimental system, especially the drumhead mode of the plate, down into the testable bandwidth. These two substructures are joined using modal constraints and two copies of the analytical fixture model (shown on the bottom left and denoted A_{an1} and A_{an2}) are removed to arrive at an estimate of the dynamic model of the built-up system, shown on the bottom right.

This same problem could have been formulated in many other ways. For example, one could use only one fixture and constrain D to A_{an} at the connection points as was done with the beam system. The procedure described in the previous paragraph was chosen instead because it preserves the experimental joint between the fixture and system B and avoids having to estimate the rotations of the connection points in the finite element model.

The physical systems are joined by eight bolts, equally spaced around the circumference of plate. Washers are used when assembling the actual hardware to assure that the systems come in contact only at these eight points, although one would expect that this isn't strictly necessary when the MCFS method is employed. The fixture was instrumented with 12 triaxial accelerometers, positioned to minimize the condition number of its mode shape matrix with 16 modes. The triax set included eight along the circumference of the ring, equally spaced between the connection points and one at the tip of each of the four tabs. This gave a mode shape matrix whose condition

number was 2.2 considering the 16 target modes. Later, additional modes were also included and found to improve the agreement between the built-up system predictions and truth data slightly in the axial direction. Eighteen modes were used in the results that follow, which gave a condition number of 5.8.

A modal test was performed on the experimental substructure, with bungee cords used to suspend the test article to simulate free boundary conditions, as shown in Fig. 8. In addition to the instrumentation on the fixture, a triaxial accelerometer was placed on the tip of the beam, and two additional uniaxial accelerometers were also mounted on the beam as shown in Fig. 8. The six rigid body modes were obtained from mass properties measurements of the parts. Twenty other elastic modes up to 4000 Hz were extracted from FRFs using the multi-reference SMAC algorithm [40, 41], resulting in a total of 26 modes for the C system. Many of these modes were bending modes of the fixture tabs. Several were bending modes of the beam on the plate. Four different hammer input locations were utilized to excite the modes. Two were in the axial and soft bending directions at the end of the beam and two were on the plate. Attempts to excite the fixture on the tabs were abandoned due to unavoidable double impacts.

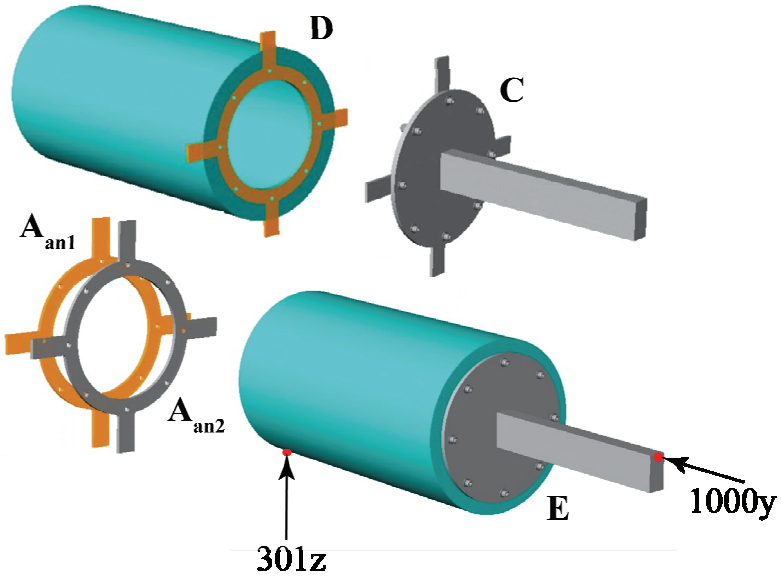

Figure 7: Schematic of Cylinder-Plate System. Labels are shown indicating the names of the subsystems, as well as two drive points where FRFs were later reconstructed.

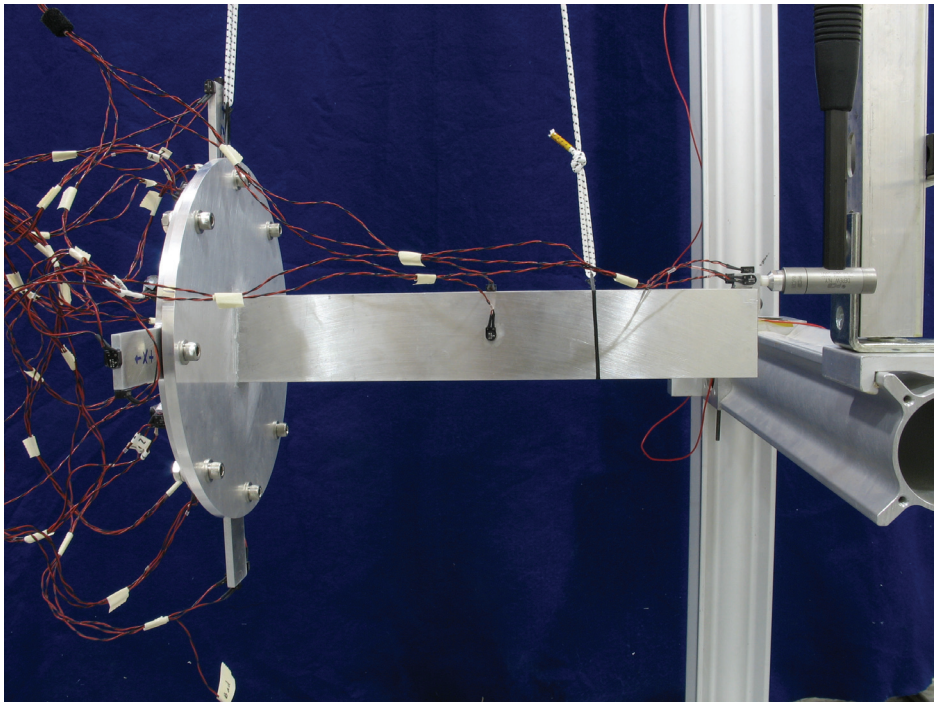

Figure 8: Photograph of Experimental substructure, modal test setup and instrumentation.

The twenty-six modes of the experimental subsystem C were combined with the 100-mode analytical model of the cylinder D and with two 18-mode models of the negative fixture A_{an}, yielding uncoupled equations of similar to what was shown in Eq. (21). The constraints for this problem consisted of MCFS constraints between the negative fixture A_{an1} and the C system, between the other negative fixture A_{an2} and the D system and between the two negative fixtures A_{an1} and A_{an2}. In each case the MCFS constraints used all 18 modes of the fixture mode shape matrix, so there were a total of 54 constraints.

$$\begin{bmatrix} \mathbf{I} & \mathbf{0} & -\boldsymbol{\Phi}_{A_{an},m}{}^{\dagger}\boldsymbol{\Phi}_{C,m} & \mathbf{0} \\ \mathbf{0} & \mathbf{I} & \mathbf{0} & -\boldsymbol{\Phi}_{A_{an},m}{}^{\dagger}\boldsymbol{\Phi}_{D,m} \\ \mathbf{I} & \mathbf{-I} & \mathbf{0} & \mathbf{0} \end{bmatrix} \begin{Bmatrix} \mathbf{q}_{A_{an1}} \\ \mathbf{q}_{A_{an2}} \\ \mathbf{q}_{C} \\ \mathbf{q}_{D} \end{Bmatrix} = \mathbf{0} \tag{24}$$

The modal parameters of the built-up system were then used to reconstruct its drive point frequency response functions at several points, two of which will be reported here. The first is located on the wall of the cylinder, measuring normal to its surface, near the end opposite where the beam is mounted, labeled 301z in Fig. 7. The second point was located at the tip of the beam, oriented axially, and was labeled 1000y, as shown in Fig. 7. The built-up system was also tested in order to validate a finite element model for the coupled-system. The finite

element truth model was found to agree very well with the measurements, so it, rather than the actual truth data, is compared with the CMS predictions in all of the following.

Figures 9 and 10 show the frequency response functions in a lateral direction and in the axial direction respectively. The FRF predicted using modal substructuring with the experimentally derived modal parameters for the C system is shown (Exper-CMS), and is compared with the FRF of the truth model (Analytical). The FRF of another model is also shown, which was similar to the Exper-CMS model except that the 26 measured modes of C were replaced with modes from a detailed finite element model. That result is denoted FEA-CMS, and gives an indication of the CMS prediction that would have been obtained if one were able to measure the modes of the C system perfectly. In the lateral direction, all three results overlay at lower frequencies, except near 160 Hz where the results are still in quite close agreement. Above 4000 Hz the CMS predictions differ considerably from the analytical truth model, but the experimental result still tracks the analytical CMS result quite closely. The agreement is also excellent in the axial direction out to about 3000 Hz, above which one would presume that the modes of the subcomponents are no longer an adequate basis for the built-up system. The Experimental results (Exper-CMS) track the FEA-CMS results very well in both Figures 9 and 10, suggesting that errors in the test do not have an important effect on the substructuring predictions for this system.

These results employed the MCFS method to join the subsystems. Additional sensors would be needed if one were to employ connection point constraints as described in Section 2.2.1 because there are a total of 48 connection point DOF, and only 36 sensors were employed on the fixture in this study. One alternative is to connect the 36 sensor DOF directly, but this provides no mechanism for averaging errors.

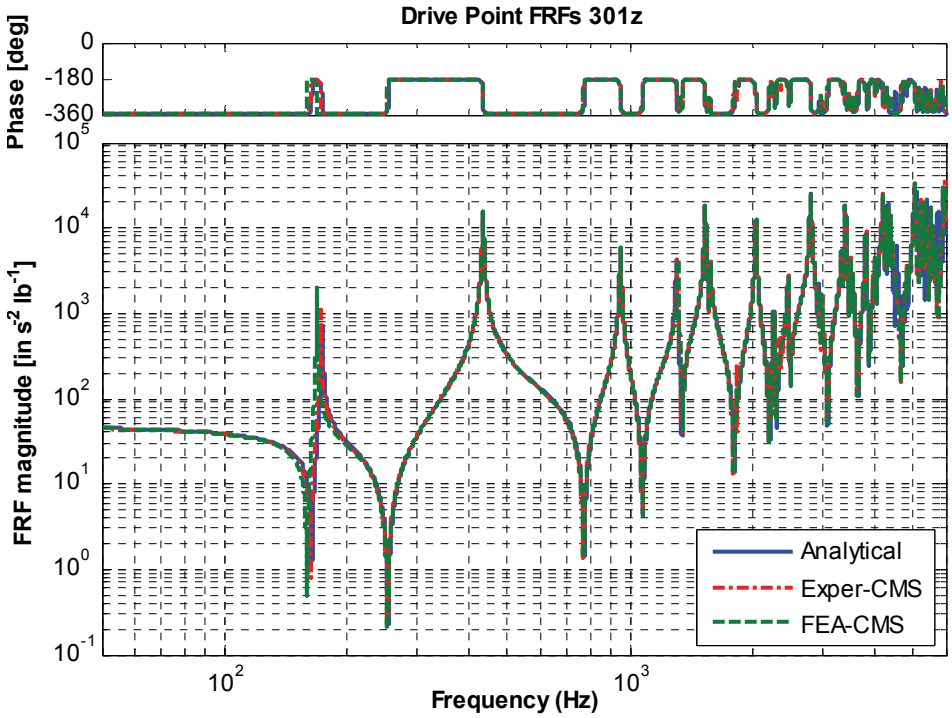

Figure 9: Drive Point Frequency Response Function at 301z (lateral direction) found in three ways, using an Analytical model (solid), using experimentally measured modal properties for the C system (dash-dot) and using a Finite element model for the C system (dashed).

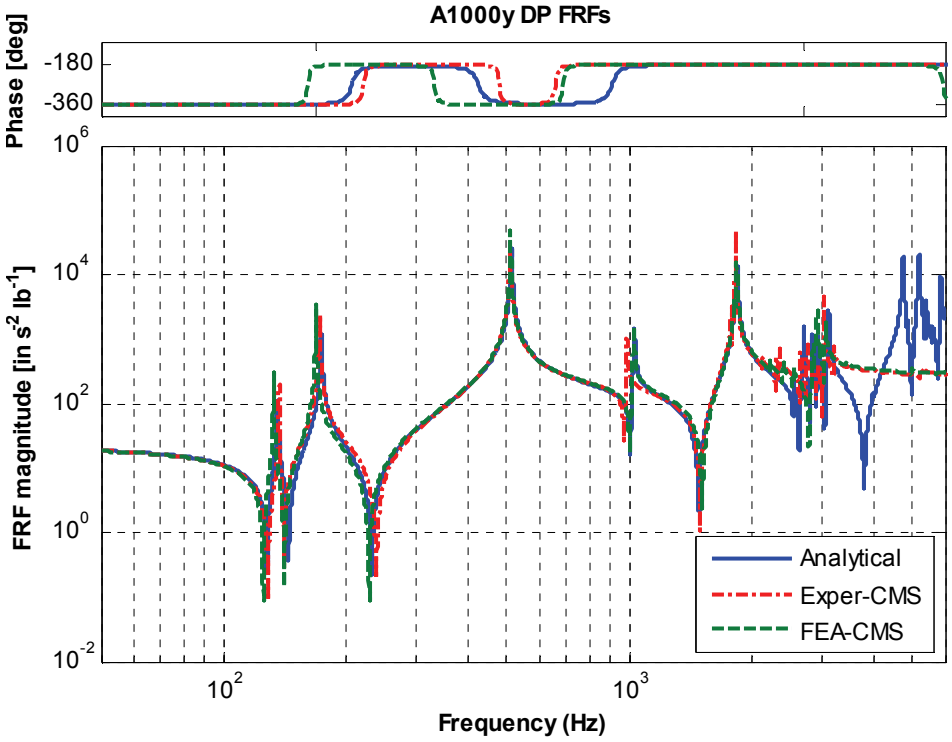

Figure 10: Drive Point Frequency Response Function at 1000y (axial direction) found in three ways, using an Analytical model (solid), using experimentally measured modal

properties for the C system (dash-dot) and using a Finite element model for the C system (dashed).

Discussion

One key to the success of the CMS procedure for this system is the fact that the fixture enriches the modal basis. In a preliminary work [16], the authors used an analytical model to show that if the fixture were not employed then the C system's natural frequencies are higher, so if the modal test is again only successful in extracting modes out to 4kHz then one obtains only 21 modes. These modes were employed in the substructuring procedure and the predictions were found to be dramatically worse than those presented here. The fixture serves to mass-load the interface to bring more modes into the testable range. This confirms that the flexible fixture produces a set of modes that are a much better basis for the experimental substructure.

It is also informative to compare the approach taken for this system with a more traditional approach. The cylinder was connected to the plate-beam at eight points. The conventional approach would treat each point as independent and require one to attach rigid masses to each to mass-load the interface and to determine the displacement and rotation. However, Baker [24] showed that this approach may not yield accurate substructuring predictions without a very large number of modes. The MCFS method was also very important for this problem. If one were to use the same flexible fixture but with connection point constraints, one would need at least 48 sensors on the fixture to capture the motions of all of the connection points rather than the 36 sensors used here. Furthermore, that problem would be ill-conditioned since the structure does not have 48 active modes in the testable bandwidth, so one would encounter dramatic sensitivity to experimental errors because the problem is underdetermined. On the other hand, using MCFS it is simple to enforce the constraint no matter how many physical connection degrees of freedom the fixture has, and one can determine whether enough were used by observing the compatibility between the substructures, as was done in Fig. 6.

4. Conclusions

This paper presented a procedure that removes the dynamic effects of a flexible fixture from a subcomponent using modal substructuring. Since modal models can be obtained experimentally using well-known procedures, this procedure could, in principle, be used to remove any dynamic subsystem from another. The approach was used here to remove the dynamics of a fixture from a subcomponent prior to joining the subcomponent in an assembly. One key to doing so in a robust manner was the way in which the constraints were applied between the actual fixture and its negative analytical model. A new method, dubbed Modal Constraints for Fixture and Subsystem (MCFS) or

simply, “modal constraints” was presented and shown to circumvent a number of difficulties. This new approach allows one to constrain the motion of two substructures at a large number of points, but in a weak or least squares sense so as to avoid high sensitivity to measurement errors.

These concepts were illustrated using both test results and finite element models for two subcomponents. The first consisted of a simple beam with the fixture attached at a single point, while the second comprised a three-dimensional structure with eight connection points. After the fixture’s dynamics were removed, each subsystem was successfully coupled to another subcomponent forming the desired assembly. Using a fixture in this way allows one to capture the rotations of the interface degrees of freedom without having to treat them explicitly, and it enriches the modal basis of the substructure, substantially improving the coupling predictions. Furthermore, since the joints between the fixture and substructures had the same material and geometry as those between the substructures in the final assembly, one would expect this approach to accurately capture the linear stiffness and damping of the joints.

Substructure uncoupling can be very sensitive to measurement errors, yet the method proposed here was successfully applied to two different systems using real test measurements, confirming that it is possible to both add and remove subcomponents using modal substructuring, even with the limitations that are inherent to all measurements.

Acknowledgments

This work was supported by, and some of this work was performed at Sandia National Laboratories. Sandia is a multi-program laboratory operated by Sandia Corporation, a Lockheed Martin Company, for the United States Department of Energy’s National Nuclear Security Administration under Contract DE-AC04-94AL85000. The authors also wish to thank the reviewers of the preliminary version of this article for their thorough reviews and the insights that they shared.

References

[1] M. Imregun, D. A. Robb, and D. J. Ewins, "Structural Modification and Coupling Dynamic Analysis Using Measured FRF Data," in *5th International Modal Analysis Conference (IMAC V)* London, England, 1987.

[2] W. Liu and D. J. Ewins, "Substructure synthesis via elastic media," *Journal of Sound and Vibration,* vol. 257, pp. 361-79, 2002.

[3] A. P. V. Urgueira, "Dynamic Analysis of Coupled Structures Using Experimental Data," PhD Thesis, *Imperial College of Science, Technology and Medicine*, London: University of London, 1989.

[4] W. J. Duncan, "The admittance method for obtaining the natural frequencies of systems," *Philosophical Magazine,* vol. 32, pp. 401-409, 1941.

[5] T. G. Carne and C. R. Dohrmann, "Improving Experimental Frequency Response Function Matrices for Admittance Modeling," in *24th International Modal Analysis Conference (IMAC XXIV)* St. Louis, Missouri, 2006.

[6] A. Kyprianou, J. E. Mottershead, and H. Ouyang, "Structural modification. Part 2: Assignment of natural frequencies and antiresonances by an added beam," *Journal of Sound and Vibration,* vol. 284, pp. 267-281, 2005.

[7] J. E. Mottershead, A. Kyprianou, and H. Ouyang, "Structural modification. Part 1: rotational receptances," *Journal of Sound and Vibration,* vol. 284, pp. 249-65, 2005.
[8] J. E. Mottershead, M. G. Tehrani, D. Stancioiu, S. James, and H. Shahverdi, "Structural modification of a helicopter tailcone," *Journal of Sound and Vibration,* vol. 298, pp. 366-84, 2006.
[9] D. de Klerk, D. J. Rixen, and S. N. Voormeeren, "General framework for dynamic substructuring: History, review, and classification of techniques," *AIAA Journal,* vol. 46, pp. 1169-1181, 2008.
[10] T.-J. Su and J.-N. Juang, "Substructure System Identification and Synthesis," *Journal of Guidance Control and Dynamics,* vol. 17, pp. 1087-95, 1994.
[11] D. R. Martinez, T. G. Carne, D. L. Gregory, and A. K. Miller, "Combined Experimental/Analytical Modeling Using Component Mode Synthesis," in *AIAA/ASME/ASCE/AHS Structures, Structural Dynamics & Materials Conference* Palm Springs, CA, USA, 1984, pp. 140-152.
[12] J. H. Ginsberg, *Mechanical and Structural Vibrations*, First ed. New York: John Wiley and Sons, 2001.
[13] R. R. J. Craig and M. C. C. Bampton, "Coupling of Substructures Using Component Mode Synthesis," *AIAA Journal,* vol. 6, pp. 1313-1319, 1968.
[14] M. S. Allen and R. L. Mayes, "Comparison of FRF and Modal Methods for Combining Experimental and Analytical Substructures," in *25th International Modal Analysis Conference (IMAC XXV)* Orlando, Florida, 2007.
[15] R. L. Mayes and E. C. Stasiunas, "Lightly Damped Experimental Substructures for Combining with Analytical Substructures," in *25th International Modal Analysis Conference (IMAC XXV)* Orlando, Florida, 2007.
[16] R. L. Mayes, P. S. Hunter, T. W. Simmermacher, and M. S. Allen, "Combining Experimental and Analytical Substructures with Multiple Connections," in *26th International Modal Analysis Conference (IMAC XXVI)* Orlando, Florida, 2008.
[17] R. H. MacNeal, "A hybrid method of component mode synthesis," *Computers & Structures,* vol. 1, pp. 581-601, 1971.
[18] S. Rubin, "Improved component-mode representation for structural dynamic analysis," *AIAA Journal,* vol. 13, pp. 995-1006, 1975.
[19] S. Goldenberg and M. Shapiro, "A study of modal coupling procedures for the space shuttle," NASA 1972.
[20] C. Yasuda, P. J. Riehle, D. L. Brown, and R. J. Allemang, "Estimation Method for Rotational Degrees of Freedom Using a Mass Additive Technique," in *2nd International Modal Analysis Conference (IMAC II)* Orlando, Florida, 1984.
[21] H. Kanda, M. L. Wei, R. J. Allemang, and D. L. Brown, "Structural Dynamic Modification Using Mass Additive Technique," in *4th International Modal Analysis Conference (IMAC IV)* Los Angeles, California, 1986.
[22] K. O. Chandler and M. L. Tinker, "General mass-additive method for component mode synthesis," in *AIAA Structures, Structural Dynamics & Materials Conference*. vol. 1 Kissimmee, FL, USA: AIAA, New York, NY, USA, 1997, pp. 93-103.
[23] C. F. Nelson and C. R. Dohrmann, "Using a modal test to estimate support properties," in *20th International Modal Analysis Conference (IMAC-XX)*. vol. 4753 II Los Angeles, CA, United States: The International Society for Optical Engineering, 2002, pp. 1417-1421.
[24] M. Baker, "Component Mode Synthesis Methods for Test-Based, Rigidly Connected Flexible Components," *Journal of Spacecraft and Rockets,* vol. 23, pp. 316-322, 1986.
[25] W. D'Ambrogio and A. Fregolent, "Decoupling procedures in the general framework of Frequency Based Substructuring," in *27th International Modal Analysis Conference (IMAC XXVII)* Orlando, Florida, 2009.
[26] E. Parloo, B. Cauberghe, F. Benedettini, R. Alaggio, and P. Guillaume, "Sensitivity-based operational mode shape normalisation: application to a bridge," *Mechanical Systems and Signal Processing,* vol. 19, pp. 43-55, 2005.
[27] J. Dong and K. G. McConnell, "Extracting multi-directional FRF matrices with "Instrument Cluster"," in *20th International Modal Analysis Conference (IMAC XX)*. vol. 4753 I Los Angeles, CA, United States: The International Society for Optical Engineering, 2002, pp. 751-764.
[28] P. Ind, "The Non-Intrusive Modal Testing of Delicate and Critical Structures," PhD Thesis, *Imperial College of Science, Technology & Medicine*, London: University of London, 2004.
[29] P. Sjovall and T. Abrahamsson, "Substructure system identification from coupled system test data," *Mechanical Systems and Signal Processing,* vol. 22, pp. 15-33, 2008.
[30] Q. Zhang, R. J. Allemang, and D. L. Brown, "Modal Filter: Concept and Applications," in *8th International Modal Analysis Conference (IMAC VIII)* Kissimmee, Florida, 1990, pp. 487-496.
[31] R. R. J. Craig, *Structural Dynamics*. New York: John Wiley and Sons, 1981.
[32] D. J. Ewins, *Modal Testing: Theory, Practice and Application*. Baldock, England: Research Studies Press, 2000.
[33] S. Maia, J. M. M. Silva, J. He, N. A. Lieven, R. M. Lin, G. W. Skingle, W. M. To, and A. P. V. Urgueira, *Theoretical and Experimental Modal Analysis*. Taunto, Somerset, England: Research Studies Press Ltd., 1997.
[34] D. C. Kammer, "Test-Analysis Model Development Using an Exact Modal Reduction," *International Journal of Analytical and Experimental Modal Analysis,* vol. 2, pp. 174-179, 1987.
[35] P. Avitabile, J. O'Callahan, C. M. Chou, and V. Kalkunte, "Expansion of rotational degrees of freedom for structural dynamic modification," in *5th International Modal Analysis Conference (IMAC V)* London, England, 1987.
[36] M. Corus, E. Balmes, and O. Nicolas, "Using model reduction and data expansion techniques to improve SDM," *Mechanical Systems and Signal Processing,* vol. 20, pp. 1067-89, 2006.
[37] P. Avitabile and J. O'Callahan, "Frequency response function expansion for unmeasured translation and rotation DOFS for impedance modelling applications," *Mechanical Systems and Signal Processing,* vol. 17, pp. 723-745, 2003.

[38] E. Balmes, "Review and evaluation of shape expansion methods," in *18th International Modal Analysis Conference (IMAC XVIII)* San Antonio, TX: Society for Experimental Mechanics Inc., USA, 2000, pp. 555-561.

[39] M. S. Allen and R. L. Mayes, "Estimating the Degree of Nonlinearity in Transient Responses with Zeroed Early-Time Fast Fourier Transforms," *Mechanical Systems and Signal Processing,* vol. http://dx.doi.org/10.1016/j.ymssp.2010.02.012, 2010.

[40] D. P. Hensley and R. L. Mayes, "Extending SMAC to Multiple Reference FRFs," in *24th International Modal Analysis Conference (IMAC XXIV)* St. Louis, Missouri, 2006.

[41] R. L. Mayes and S. E. Klenke, "The SMAC Modal Parameter Extraction Package," in *17th International Modal Analysis Conference* Kissimmee, Florida, 1999, pp. 812-818.